

Simulation of phonon-induced mobility under arbitrary stress, wafer and channel orientations and its application to FinFET technology

Kai Xiu* and Phil Oldiges

IBM Semiconductor Research and Development Center (SRDC), 2070 Route 52, Hopewell Junction, NY 12533

*Email: kaixiu@us.ibm.com

Abstract—By applying appropriate tensor transformations for the subband solutions of electron and hole and their transport properties, we demonstrated the capability of determining the phonon induced mobility for planar and FinFET MOSFET devices under arbitrary stress, wafer and channel orientations. The electron and hole mobilities for such devices are numerically solved and their angular dependences on wafer are shown. We further investigated the mobility trend under some high index gate orientation conditions that are of interest to current 14 nm FinFET technology

Keywords: mobility, tensor, electron, hole, sidewall, phonon, orientation, stress, FinFET

I. INTRODUCTION

Conventional planar MOSFET has been a dominant player in the past decades due to its apparent manufacturability and adaptability to Moore's Law. To keep up with the technology's scaling trend stress had been introduced as an important leverage to boost the performance. In recent years, non-planar devices based on multiple gate structure, i.e. FinFET (also known as Tri-Gate), appeared to become the candidate for the 14nm node and beyond. TCAD-wise, there are multifold complications due to the introduction of stress on a non-planar gate structure: the silicon wafer is an anisotropic material whose set of elastic coefficients follow the rule tensor transformation for any given orientation of interest, while the Hamiltonian that describes the carrier transport in the channel region also transforms accordingly – in the case of FinFET a non-vertical sidewall due to process constraint can give rise to a high index channel orientation. It is thus a necessity to extend the TCAD capability of describing carrier transport beyond the traditional planar wafer/channel combination of (100)/[110]. In this manuscript, we present a generalized TCAD framework which covers the treatment of such general orientations and show their effect on phonon-limited mobility in the inversion channel under the presence of arbitrary stress.

II. GENERAL FORMULATION

To calculate the subbands for a non-trivial wafer/channel orientation, we first establish the linkage between the crystal principle coordinate system (PS) and the local laboratory coordinate system (LS), upon which appropriate transformation of strain tensor, effective mass tensor, as well as Hamiltonian and general k-vector in the calculation of hole subbands can be established. In the case of electrons, we take the assumption of

an isotropic and parabolic conduction band with their effective masses depending on the valley orientation. For an arbitrary wafer orientation $(l_i m_i n_i)$, and transport direction $[l_i m_i n_i]$, and for any given valley, the effective mass tensor in LS and PS takes the general form

$$\tilde{W} = \begin{pmatrix} \tilde{w}_{11} & \tilde{w}_{12} & \tilde{w}_{13} \\ \tilde{w}_{12} & \tilde{w}_{22} & \tilde{w}_{23} \\ \tilde{w}_{13} & \tilde{w}_{23} & \tilde{w}_{33} \end{pmatrix} \quad \text{and} \quad W = \begin{pmatrix} w_{11} & 0 & 0 \\ 0 & w_{22} & 0 \\ 0 & 0 & w_{33} \end{pmatrix} \quad (1)$$

By introducing the rotation matrix R linking these two coordinate systems we can express their tensor transformation as

$$\tilde{W} = RWR^T \quad \text{where} \quad R = \begin{pmatrix} l_1 & m_1 & n_1 \\ l_2 & m_2 & n_2 \\ l_3 & m_3 & n_3 \end{pmatrix} \quad (2)$$

Note that $m_{ii}=1/w_{ii}$ is the longitudinal or transverse effective mass in this valley, $(l_i m_i n_i)$, is the (normalized) directional cosine for channel, transverse and quantization directions. In order to reduce the Schrodinger equation to an equation with a single variable, we follow the transformation [1] which gives rise to two diagonal and one cross term of the effective masses in the free plane

$$\begin{aligned} w_{11}' &= \tilde{w}_{11} - \tilde{w}_{12}^2 / \tilde{w}_{33} \\ w_{22}' &= \tilde{w}_{22} - \tilde{w}_{23}^2 / \tilde{w}_{33} \\ w_{12}' &= 2(\tilde{w}_{12} - \tilde{w}_{13}\tilde{w}_{23} / \tilde{w}_{33}) \end{aligned} \quad (3)$$

Eventually the energy dispersion for subband i becomes

$$E_i(k_1, k_2) = E_i' + \frac{\hbar^2}{2} (w_{11}' k_1^2 + w_{12}' k_1 k_2 + w_{22}' k_2^2) \quad (4)$$

where the eigenvalue E_i' is the solution of Schrodinger equation

$$\frac{\tilde{w}_{33}\hbar^2}{2} \frac{d^2\phi_i(z)}{dz^2} + eV(z) = E_i'\phi_i(z) \quad (5)$$

The subbands of the conduction band are solved under a triangle shaped effective electrostatic potential $V(z)$ as appeared in (5), and (6) for the valence band – this non-self-consistency is a reasonable approximation when the gate voltage is in the small to medium range, which is of our most interest.

The calculation of subbands of hole valence bands involves the perturbation over a 6-fold degenerated (taking spin-orbit coupling into consideration) Schrodinger equation

$$\left[\widetilde{H}(K, k_z) + I V(z) \right] \psi_K(z) = E(K) \psi_K(z) \quad (6)$$

in which $K = (k_1, k_2)$ is the two free k -components, I is the 6x6 identity matrix. In the crystal principle coordinate system the Hamiltonian H takes the form

$$H(k) = H_{so} + \begin{pmatrix} H_{kp} & 0 \\ 0 & H_{kp} \end{pmatrix}, \quad H_{so} = \frac{\delta_0}{3} \begin{pmatrix} 0 & -I & 0 & 0 & 0 & 1 \\ I & 0 & 0 & 0 & 0 & -I \\ 0 & 0 & 0 & -1 & I & 0 \\ 0 & 0 & -1 & 0 & I & 0 \\ 0 & 0 & -I & -I & 0 & 0 \\ 1 & I & 0 & 0 & 0 & 0 \end{pmatrix} \quad (7)$$

$$H_{kp}(k) = \begin{pmatrix} l k_x^2 + m (k_y^2 + k_z^2) & n k_x k_y + n_1 e_{xy} & n k_x k_z + n_1 e_{xz} \\ +l_1 e_{xx} + m_1 (e_{yy} + e_{zz}) & & \\ n k_x k_y + n_1 e_{xy} & l k_y^2 + m (k_x^2 + k_z^2) & n k_y k_z + n_1 e_{yz} \\ +l_1 e_{yy} + m_1 (e_{xx} + e_{zz}) & & \\ n k_x k_z + n_1 e_{xz} & n k_y k_z + n_1 e_{yz} & l k_z^2 + m (k_x^2 + k_y^2) \\ +l_1 e_{zz} + m_1 (e_{xx} + e_{yy}) & & \end{pmatrix}$$

Here H_{kp} and H_{so} are standard kp and spin-orbit matrix forms of Hamiltonian for silicon valence band [2,3], in which e_{xx} , e_{yy} , e_{zz} , e_{xy} , e_{xz} , e_{yz} are strain tensor components, all expressed in PS. By using the matrix R defined in (2) that links the rotational transformation between LS and PS, we obtain the rotated k -vectors

$$\tilde{k} = Rk \quad (8)$$

and replace them into H . As the final step the perpendicular k_z is replaced by differential operator $k_z \rightarrow -i\nabla$ and discretized for the numerical solution.

Finally, the ‘‘local’’ mechanical properties including the Young’s modulus and Poisson’s ratio are all obtained according to the appropriate tensor transformation rules [4]. Their values are used to generate corresponding strain tensor in the LS which is eventually transformed into the PS.

III. MOBILITY

Carrier scattering with both intra-valley acoustic phonon and inter-valley non-polar optical phonon are considered in our calculation, where we assumed the phonon deformation potential as well as scattering that appear in the relaxation time to be isotropic [3]:

$$\frac{1}{\tau_{AC}^{\alpha,i}(\mathbf{k})} = \frac{2\pi k_B T \Xi_{eff}^2}{\hbar \rho v_i^2} \sum_{\beta} F_{\alpha\beta} \rho_{\alpha} [E^{\beta,i}(\mathbf{k})] \quad (9)$$

$$\frac{1}{\tau_{op}^{\alpha,i}(\mathbf{k})} = \frac{\pi D_{op}^2}{\rho \omega_{op}} \sum_{\beta} F_{\alpha\beta} \rho_{\alpha} [E^{\beta,i}(\mathbf{k}) \mp \hbar \omega_{op}]$$

$$\times \frac{1 - f_0 [E^{\beta,i}(\mathbf{k}) \mp \hbar \omega_{op}]}{1 - f_0 [E^{\beta,i}(\mathbf{k})]} \left(n_{op} + \frac{1}{2} \pm \frac{1}{2} \right)$$

The individual mobility contribution from each valley α and subband i can be expressed as the Kubo-Greenwood

formula which is chiefly determined by the group velocity v and relaxation time τ in the 2D momentum space [3]:

$$\mu_{xx}^{\alpha,i} = \frac{2e}{n^{\alpha,i} \hbar} \int \frac{d^2 k}{(2\pi)^2} v_x^{\alpha,i}(k) \tau_x^{\alpha,i}(k) \frac{\partial f^{\alpha,i}(k)}{\partial k_x} \quad (10)$$

In the case of electron the above expression can largely reduced by assuming a parabolic band approximation

$$\mu_{xx}^{\alpha,i} = \frac{2ge m_{dos}}{n^{\alpha,i} \pi \hbar^2 m_c} \int_{E_0}^{\infty} (E - E_0) \tau^{\alpha,i}(E) \frac{\partial f^{\alpha}(E)}{\partial E} dE \quad (11)$$

IV. APPLICATION TO PLANAR DEVICE

As our first application, we show the angular dependence of phonon-induced mobility of a planar device on a (001) wafer and a (110), whose top view schematics are shown in Fig. 1, under the influence of a single source of local stress (i.e. stress tensor is diagonal in the local laboratory coordinate system). The mobility under various stress condition is plotted against the polar angle on the wafer as shown in Figs (3-6). The zero angle corresponds to the (100) channel direction on the (001) wafer and [1-10] direction on the (110) wafer. The effects of local stress are shown separately for three distinct cases: a longitudinal (s_{xx}), transverse (s_{yy}) and vertical (s_{zz}) components ranging up to 0.6 GPa. These are typical values from a TCAD process simulation.

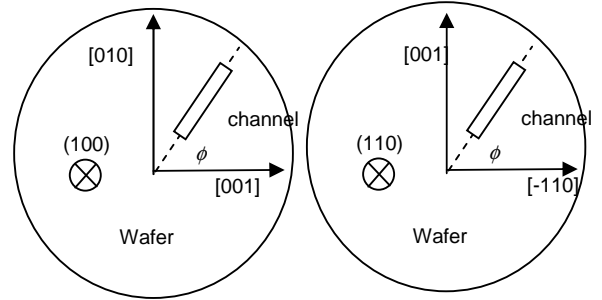


Fig.1 Top view of a conventional planar MOSFET oriented on a (100) wafer and (110) wafer with a arbitrary angle ϕ versus the notch direction ([001] for a (100) wafer and [-110] for a (110) wafer

The results of electron mobility on a (001) wafer come at no surprise: it maintains a relatively isotropic behavior and shows enhancement under tensile stresses along the longitudinal and transverse direction, and under compressive stress along the vertical direction. The electron mobility on (110) wafer, on the other hand, shows a cross-over of orientation which flips the stress effect for all the separate stress cases. In the situation of hole transport, we see the familiar enhancement under a longitudinal compressive stress along the [110] direction as indicated in the first graph in Fig. 5. The stress effect diminishes as the device is rotated away from this orientation. In the case of a (110) wafer for hole transport, we see that both the ‘‘relaxed’’ mobility and enhancement happen at the nominal [1-10] channel direction, while the 45 degree rotated direction [111’] (a high index case) shows a lesser moderate enhancement.

V. APPLICATION TO FINFET DEVICE

In this section we will study a generalized mobility behavior of a FinFET device as seen in Fig. 2. In the left view we show the schematics of the FinFET device on a (001) wafer with an arbitrary channel orientation angle. In contrast to a planar device its channel direction is parallel to the wafer plane. In the right view the FinFET can be seen featuring a non-vertical sidewall due to process variation.

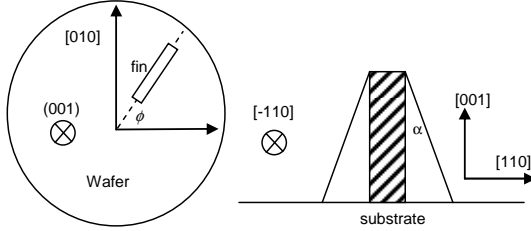


Fig.2 Top and cross-section views of a FinFET on a (001) wafer. α is defined as the angle between the normal vector to the wafer plane (001) and fin sidewall

As in the planar case we consider the effect of local stress for two distinct cases: a longitudinal s_{xx} and a transverse s_{zz} components ranging up to 0.6 GPa. In our first example as shown in Fig. 7, we assume the fin sidewall to be ideally vertical, and study the mobility's angular dependence on channel orientation angle ϕ . In the case of electron we see moderate enhancement in the [110] direction, marked in bold black arrow at 45 degree, for applied longitudinal tensile stress. We can also find a slight degradation for a compressive transverse stress. In the situation of hole transport, we see the preferred intrinsic mobility as well as the enhancement direction both occur in [110] and they drop rapidly as the device is rotated away from it. As our second demonstration, we study the [110] intrinsic mobility behavior when FinFET has a slant sidewall, in other words, the FinFET channel direction is confined in the [110] ($\phi = \pi/4$ in Fig. 2) while α deviates from zero as shown in right view of Fig. 2. It should be noted that under such circumstance the normal vector to the inversion channel will move from [110] into some high index directions and eventually coincide with the wafer normal direction [001] if the slope angle α is allowed to reach 90 degree, technically a planar device, as indicated in Fig.1 and Fig. 2. We plot the mobility as a function of sidewall slope α for nFET and pFET in Fig. 8. We can see the hole mobility degrades rapidly with increasing α , namely, $\sim 20\%$ if the sidewall angle is off vertical by 15 degrees in the early stage. On the other hand the electron mobility is not much affected by non-vertical sidewalls, featuring just a moderate rise.

VI. CONCLUSION

In conclusion, we have demonstrated that the calculation of mobility for an arbitrary stress/wafer/channel orientation is feasible by properly applying the tensor transformation of inverse mass tensor for the electron and k-vector space for the holes for planar and FinFET devices with non-trivial channel and stress orientations. Such a methodology has enabled us to show the trend of mobility under different level of stress while

the device is rotated on a wafer with specific orientation, and enhanced our TCAD capability for quantitatively predicting the benefits of future stress technologies.

REFERENCES

- [1] F. Stern and W. E. Howard, Phys. Rev., 163, 816 (1967)
- [2] M. V. Fischetti and S. Laux, J. Appl. Phys., 85, 7984 (1996)
- [3] M. V. Fischetti et al, J. Appl. Phys., 94, 1079 (2003)
- [4] W. A. Brantley, J. Appl. Phys., 44, 534 (1973)

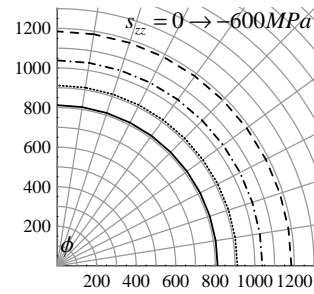
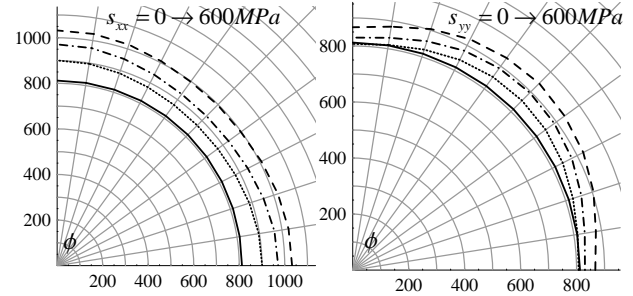


Fig.3 Mobility (cm^2/Vs) polar plot as a function of orientation angle and three various stress levels (the increasing trend is represented by solid line-dotted line-dashed dotted line-dashed line) for the (001)/[100] nFET. Upper left: longitudinal stress only; Upper right: transverse stress only; Lower left: vertical stress only

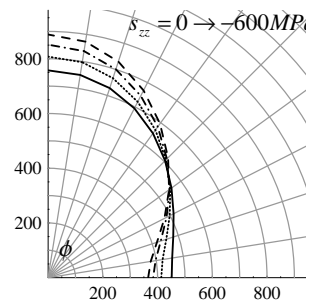
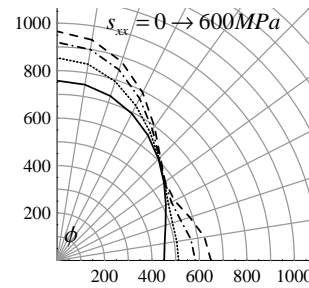


Fig.4 Mobility (cm^2/Vs) polar plot as a function of orientation angle and three various stress levels (the increasing trend is represented by solid line-dotted line-dashed dotted line-dashed line) for the (110)/[1-10] nFET. Upper left: longitudinal stress only; Upper right: transverse stress only; Lower left: vertical stress only

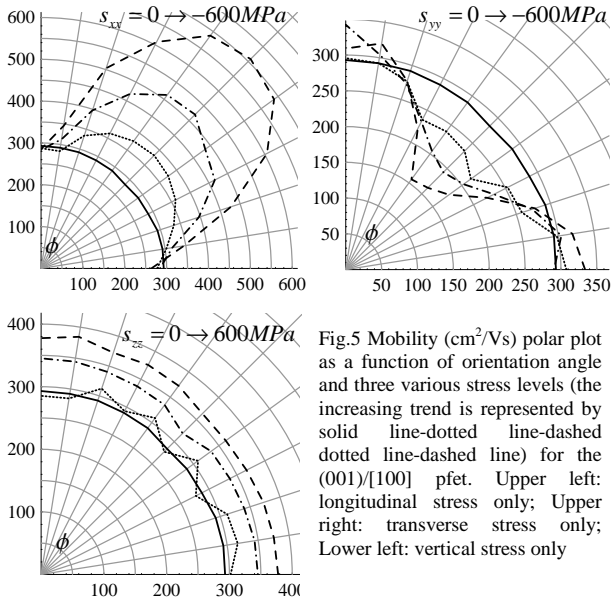


Fig. 5 Mobility (cm^2/Vs) polar plot as a function of orientation angle and three various stress levels (the increasing trend is represented by solid line-dotted line-dashed dotted line-dashed line) for the (001)/[100] pFET. Upper left: longitudinal stress only; Upper right: transverse stress only; Lower left: vertical stress only

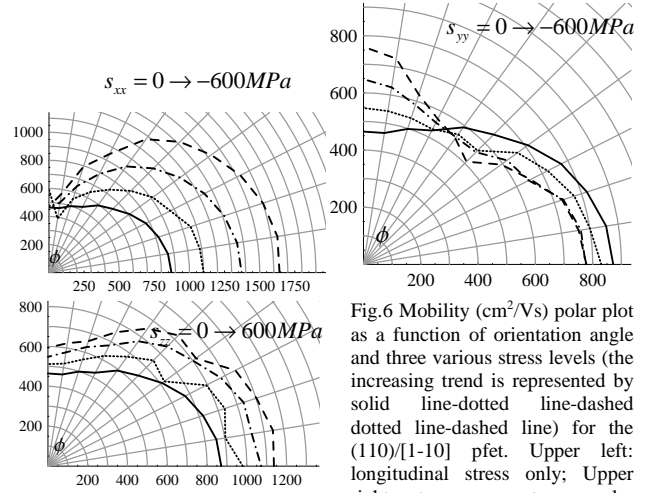


Fig. 6 Mobility (cm^2/Vs) polar plot as a function of orientation angle and three various stress levels (the increasing trend is represented by solid line-dotted line-dashed dotted line-dashed line) for the (110)/[1-10] pFET. Upper left: longitudinal stress only; Upper right: transverse stress only; Lower left: vertical stress only

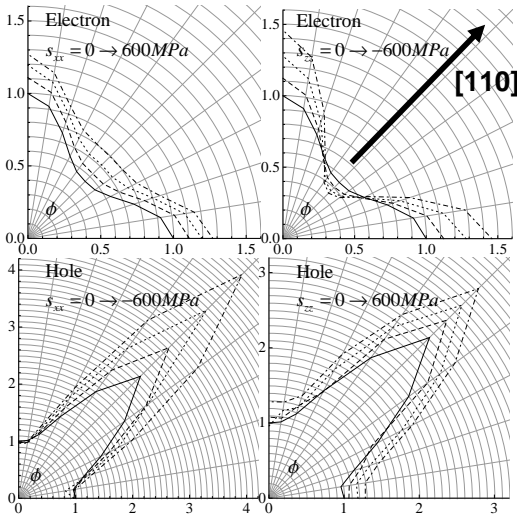


Fig. 7 Mobility polar plot as a function of orientation angle and two separate stress sources. As shown in Fig. 2 the fin's transport direction is aligned as ϕ -angle versus the [100] direction on wafer. Mobility values are shown as scaled by the relaxed mobility of [001] direction for electron and hole respectively. Left: longitudinal stress (tensile for nFET and compressive for pFET). Right: transverse stress (compressive for nFET and tensile for pFET). The increasing trend is represented by solid (no stress); dashed (200 in magnitude) dotted (400 in magnitude) and dashed dotted line (600 in magnitude) for the (001) wafer FinFET

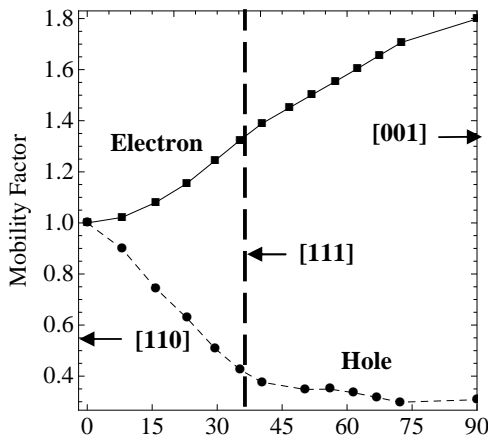


Fig. 8 Varying trend of mobility factor as a function of sidewall angle α as shown in Fig. 2, expressed as its value divided by its nominal $\alpha=0$ counterpart respectively for nFET (solid line) and pFET (dashed line); As α increases from zero to 90 degree, the channel surface will pass through [110], [111] and [001], as indicated in the figure